RESEARCH MEMORANDUM

PRELIMINARY LOW-SPEED WIND-TUNNEL INVESTIGATION OF SOME ASPECTS OF THE AERODYNAMIC PROBLEMS ASSOCIATED WITH MISSILES CARRIED EXTERNALLY IN POSITIONS NEAR AIRPLANE WINGS

By William J. Alford, Jr., H. Norman Silvers,
and Thomas J. King, Jr.

Langley Aeronautical Laboratory
Langley Field, Va.

NATIONAL ADVISORY COMMITTEE
FOR AERONAUTICS

WASHINGTON

December 27, 1954

NACA RM L54J20

[redacted]

NATIONAL ADVISORY COMMITTEE FOR AERONAUTICS

RESEARCH MEMORANDUM

PRELIMINARY LOW-SPEED WIND-TUNNEL INVESTIGATION OF SOME ASPECTS OF THE AERODYNAMIC PROBLEMS ASSOCIATED WITH MISSILES CARRIED EXTERNALLY IN POSITIONS NEAR AIRPLANE WINGS

By William J. Alford, Jr., H. Norman Silvers, and Thomas J. King, Jr.

SUMMARY

A low-speed wind-tunnel investigation has been made of some aspects of the aerodynamic problems associated with the use of air-to-air missiles when carried externally on aircraft. Measurements of the forces and moments on a missile model for a range of positions under the midsemispan location of a 45° sweptback wing indicated longitudinal and lateral forces and moments of sufficient magnitude to present possible serious problems with regard to both carriage and release of the missiles. Surveys of the characteristics of the flow field in the region likely to be traversed by the missiles showed abrupt gradients in both flow angularity and in local dynamic pressure. Through the use of aerodynamic data on the isolated missile and the measured flow-field characteristics, the longitudinal forces and moments acting on the missile while in the presence of the wing-fuselage combination could be estimated with fair accuracy. Although the lateral forces and moments predicted were qualitatively correct, there existed some large discrepancies in absolute magnitude.

INTRODUCTION

A number of problems have arisen in connection with the use of stores or missiles that are carried externally on aircraft. These problems involve the loads acting on the bodies while they are being carried or the influence of the loads on the paths taken by the bodies released from the aircraft while in flight. (See refs. 1 and 2.) In general, all of these problems are related to the nonuniform field of flow generated by an airplane. Because of the complexity of the flow, the investigations that have been reported (refs. 3 to 5) have yielded little

[redacted]

information suitable for generalized interpretation of nonuniform flow fields and their effects on missile launching behavior.

The National Advisory Committee for Aeronautics is making studies of the flow fields about wing-body combinations in order to provide fundamental information applicable to the use of external stores and missiles. As a part of this program, the present paper presents some results of a low-speed wind-tunnel investigation of problems associated with the launching of air-to-air missiles from an airplane configuration having a sweptback wing. Included in the paper are results of flow-field surveys at the midsemispan location, results of measurements of forces and moments on a missile model at various locations within the field surveyed, and results of some calculations that indicate the degree of accuracy with which the missile forces and moments can be computed when the free-air characteristics of the missile and the characteristics of the flow field are known.

SYMBOLS

C_N	missile normal-force coefficient, $\frac{\text{Normal force}}{q_0 S_m}$
C_m	missile pitching-moment coefficient, $\frac{\text{Pitching moment}}{q_0 S_m \bar{c}_m}$
C_Y	missile side-force coefficient, $\frac{\text{Side force}}{q_0 S_m}$
C_n	missile yawing-moment coefficient, $\frac{\text{Yawing moment}}{q_0 S_m b_m}$
C_L	lift coefficient, $\frac{\text{Lift}}{q_0 S}$
q_0	free-stream dynamic pressure, lb/sq ft
q_l	local dynamic pressure, lb/sq ft
V_0	free-stream velocity, ft/sec
S_m	exposed area of two missile wing panels, 0.046 sq ft
S	wing area, 6.25 sq ft
c	local wing chord of wing-fuselage combination, ft

[redacted]

$\bar{c}_m$	mean aerodynamic chord of exposed missile-wing area, 0.189 ft
b_m	span of missile wing, 0.415 ft
b	span of wing-fuselage combination, 5 ft
x	distance from leading edge of the local wing chord to missile center of gravity, positive rearward (fig. 1), ft
y	spanwise distance from fuselage center line, positive right (fig. 1), ft
z	vertical distance to missile center line above wing chord plane, positive up (fig. 1), ft
d_m	diameter of missile body, 1.08 in.
α	geometric angle of attack (fig. 2), deg
β	angle of sideslip (fig. 2), deg
α_l	resultant flow angularity induced by wing-fuselage combination (fig. 2), measured in xz-plane, between local flow direction and missile model axis of symmetry, $\alpha_l = \alpha - \epsilon$, deg
β_l	resultant flow angularity induced by wing-fuselage combination (fig. 2), measured in xy-plane, between local flow direction and missile model axis of symmetry, $\beta_l = \beta + \sigma$, deg
ϵ	downwash angle induced by wing-fuselage combination (fig. 2), measured in xz-plane between free-stream flow direction and local flow direction; positive when local flow is inclined downward relative to free stream, deg
ϵ_{W_e}	effective downwash angle induced by missile wing on missile tail (fig. 2), positive down, deg
σ	sidewash angle induced by wing-fuselage combination (fig. 2), measured in xy-plane between free-stream flow direction and local flow direction; for region on left side of airplane model plane of symmetry, positive sidewash corresponds to outward inclination of local flow relative to free stream, deg

[redacted]

σ_{W_e} effective sidewash angle induced by missile wing on missile tail (fig. 2), positive outboard for left wing panel, deg

$C_{N_\alpha} = \frac{\partial C_N}{\partial \alpha}$, per deg

$C_{m_\alpha} = \frac{\partial C_m}{\partial \alpha}$, per deg

$C_{Y_\beta} = \frac{\partial C_Y}{\partial \beta}$, per deg

$C_{n_\beta} = \frac{\partial C_n}{\partial \beta}$, per deg

Subscripts:

B missile body

W missile wing

T missile tail

e effective value

MODELS AND APPARATUS

The wing of the wing-fuselage combination had the quarter-chord line swept back 45°, an aspect ratio of 4, a taper ratio of 0.3, and NACA 65A006 airfoil sections parallel to the plane of symmetry. The fuselage consisted of an ogival nose section, a cylindrical center section, and a truncated tail cone. A two-view drawing of the wing-fuselage combination as part of the test setup is shown in figure 1, and the fuselage ordinates are presented in table I.

The angularity and dynamic pressure surveys were made simultaneously with a rake of six hemispherical-headed probes utilizing both pitch- and yaw-angle orifices in combination with a pitot-static arrangement for measuring dynamic pressure. A photograph of the angularity rake installed on the wing-fuselage combination is presented as figure 3.

The missile used in the force and moment phase of the investigation was a model of an air-to-air guided missile with an ogival nose, a

[redacted]

cylindrical body, delta wings, and 45° pointed tail fins. The missile was internally instrumented with a strain-gage balance and was sting-mounted from the rear of the wing-fuselage combination. The arrangement of the missile in relation to the wing-fuselage combination is shown in figures 1 and 4 and its general dimensions are presented in figure 5.

TESTS AND RESULTS

The tests were made in the Langley 300 MPH 7- by 10-foot tunnel at a velocity of 100 miles per hour and included surveys of the flow angularity and dynamic pressure in the vicinity of the wing-fuselage combination, force and moment measurements on the missile model when located at various positions within the wing-fuselage flow field, and breakdown tests of the isolated missile. This paper presents experimental results at angles of attack of -0.2°, 3.8°, and 8.2° at 0° sideslip.

The angularity and dynamic pressure data are presented in contour form for the wing midsemispan position. The contours of local angularity values are presented relative to the wing chord line and hence include measurements of the geometric angle plus the induced angles generated by the wing-fuselage combination.

The surveys were made over the right wing with the wing-fuselage model inverted to avoid support-strut interference and therefore represent conditions under the left wing of the model. Since the missile model was not in place, the surveys do not include mutual interference effects.

Force and moment characteristics measured on the missile while in the presence of the wing-fuselage combination are presented in the figures along with the angularity contours in order to facilitate analysis of the results. The positive directions of the forces and moments measured on the missile model are shown in figure 2.

The results of breakdown tests of the isolated missile are presented as variations of normal force and pitching moment with angle of attack, but also are applicable as variations of side force and yawing moment with angle of sideslip if proper consideration is given to the definition of coefficients and to the sign convention.

Jet-boundary corrections calculated by the method of reference 6, along with a free-stream misalinement angle of 0.2°, have been applied to the angle of attack when the wing-fuselage combination influenced the test results. In the case of the isolated-missile tests, only the misalinement correction was applied. Jet-boundary corrections were not applied to the flow angularity results since these corrections were

[redacted]

within the expected accuracy limits of the flow-angularity measurements. Blockage corrections calculated by the method of reference 7 were applied to the dynamic pressure.

Consideration of the angularity-rake calibration, the method of rake support, and the data-reduction procedure indicates that the angular values presented are accurate to within $\pm 0.5^{\circ}$. Consideration of the missile model strain-gage balance calibrations and the general repeatability of the data indicates that the accuracy of missile-alone force and moment components are approximately accurate within the following limits:

Coefficient	Error
C_N	± 0.02
C_m	± 0.02
C_Y	± 0.02
C_n	± 0.01

DISCUSSION

The longitudinal angularity contours are presented in parts (a) and the lateral angularity contours are presented in parts (b) of figures 6 to 8. Also included in figures 6 to 8 are the force and moment characteristics of the missile model in the presence of the wing-fuselage combination. The local dynamic pressure ratios are presented in figure 9 for three angles of attack. The normal-force and pitching-moment characteristics of the isolated missile are presented in figure 10 and the effective downwash characteristics of the isolated missile are shown in figure 11. A comparison between the measured and estimated forces and moments on the missile in the presence of the wing-fuselage combination is presented in figure 12.

Wing-Fuselage Angularity Characteristics

The longitudinal angularity contours (parts (a) of figs. 6 to 8) indicate the presence of both chordwise and vertical gradients near zero angle of attack with these gradients becoming generally larger as the geometric angle is increased. Positions where the local angularity exceeds the geometric angle indicate regions of upwash and, conversely, positions where the local angularity is less than the geometric angle are regions of downwash. The most severe gradients are seen to exist above the wing chord plane for positive angles of attack.

The lateral angularity contours (parts (b) of figs. 6 to 8) also indicate both vertical and longitudinal gradients. With the sign convention adopted, positive values of local angularities indicate a flow to the left when viewed from the rear. Inasmuch as these surveys were made about the left wing panel, positive angles indicate an outflow direction (flow toward tip). It should also be noted that these tests were made at 0° sideslip. These lateral flow directions could then be attributed to the effects of wing sweep and thickness taper for the near zero angle-of-attack case (fig. 6(b)) and to a combination of the aforementioned effects with lift-induced sidewash for the lifting condition (figs. 7(b) and 8(b)). Examination of the lateral angularity contours indicates that, near zero angle of attack, the direction of the flow is inboard. At positive angles of attack, the flow direction below the wing-chord plane is predominantly in an outboard direction, and above the chord plane the flow direction is inward. These results pertain to regions outside the wing boundary layer and hence have characteristics considerably different from those that would be expected close to the wing surface.

Missile Force and Moment Characteristics in Presence of Wing-Fuselage Combination

Presented on the same plots and using the same abscissas as the angularity contours (figs. 6 to 8) are the force and moment characteristics of the missile when it is in the wing flow field. The longitudinal lines in the angularity contours identified as A and B are the paths along which the missile was translated. Line A is 15.5 percent of the local wing chord below the wing-chord plane and line B is 37.2 percent of the local wing chord below the wing-chord plane. The missile force and moment characteristics are presented as functions of the chordwise positions of the missile center of gravity relative to the leading edge of the wing chord. (See fig. 6(a).) Also presented in figures 6 to 8 are the isolated-missile force and moment levels, from figure 10, to show the degree of induced deviation.

The missile pitching moment and normal force (parts (a) of figs. 6 to 8) are seen to have large deviations from the respective levels of the isolated missile even near zero angle of attack. As would be expected, these variations diminish as the missile is displaced from the wing-chord plane and tend to their free-stream level sufficiently far ahead of the wing.

The yawing moments induced on the missile due to the proximity of the wing-fuselage combination (parts (b) of figs. 6 to 8) are seen to be comparable in magnitude to the pitching moments when consideration is given to the nondimensionalizing parameters of these respective coefficients.

[redacted]

Brief studies using these data in conjunction with the equations of motion indicated that these forces and moments, both longitudinal and lateral, are of sufficient magnitude to present possible serious problems with regard to carriage and release of the missiles.

Dynamic Pressure Characteristics

The local dynamic pressure ratios in the field surrounding the wing (fig. 9) indicate that even the relatively thin airfoil section employed (NACA 65A006) generates sizeable disturbances in the air stream at essentially zero angle of attack. As the angle is increased, the lift effect on the dynamic-pressure ratios soon predominates over the thickness effect. The existence of these dynamic pressure gradients is another factor that must be considered in analyzing and in attempting to predict the missile characteristics.

Isolated-Missile Force and Moment Characteristics

The normal-force and pitching-moment characteristics of the isolated missile and its component parts as determined from breakdown tests in the free stream are shown in figure 10. By virtue of the missile symmetry, these data are also applicable as side-force and yawing-moment characteristics, considering the appropriate dimensions and signs.

The slopes of the normal-force and pitching-moment curves of the isolated-missile component parts were measured at zero angle of attack and are presented, along with the lateral parameters that would be obtained if the tests were made at angles of sideslip, and are listed below:

$$\left(C_{N_\alpha}\right)_B = -\left(C_{Y_\beta}\right)_B = 0.0075$$

$$\left(C_{N_\alpha}\right)_{BT} = -\left(C_{Y_\beta}\right)_{BT} = 0.0413$$

$$\left(C_{N_\alpha}\right)_{BW} = -\left(C_{Y_\beta}\right)_{BW} = 0.0836$$

$$\left(C_{m_\alpha}\right)_B = 0.0137$$

$$\left(C_{m_\alpha}\right)_{BT} = -0.125$$

$$\left(C_{m_\alpha}\right)_{BW} = 0.064$$

[redacted]

$$\left(C_{n_\beta}\right)_B = -\frac{\bar{c}_m}{b_m}\left(C_{m_\alpha}\right)_B = -0.00624$$

$$\left(C_{n_\beta}\right)_{BT} = -\frac{\bar{c}_m}{b_m}\left(C_{m_\alpha}\right)_{BT} = 0.0569$$

$$\left(C_{n_\beta}\right)_{BW} = -\frac{\bar{c}_m}{b_m}\left(C_{m_\alpha}\right)_{BW} = -0.0291$$

In order to determine an effective downwash angle at the missile tail, as affected by the missile wing, incremental pitching moments of the missile configurations utilizing the tail, with the wing both on and off, are presented in figure 11. The difference in angle at a constant pitching-moment increment is an effective downwash angle at the missile tail. This downwash angle is referred to as an effective value, since the change in dynamic pressure at the missile tail due to the missile wing is, for these tests, unknown. By virtue of the missile symmetry, these angles are equal in magnitude but of opposite sign from the side-wash angle, if considered from a lateral-plane standpoint.

Estimation of Missile Characteristics in the Presence of the Wing-Fuselage Combination

The results of an attempt to estimate the forces and moments on the missile while in the presence of the wing-fuselage combination are presented for comparison with the experimental data in figure 12. These estimations were made using the isolated missile characteristics from the breakdown tests (figs. 10 and 11), the angularity results (figs. 6 to 8), and dynamic pressure contours (fig. 9) in the following equations:

$$\left(C_N\right)_{total} = \left(C_{N_\alpha}\right)_B \alpha_{l_B}\left(\frac{q_l}{q_0}\right)_B + \left(C_{N_\alpha}\right)_{BW-B} \alpha_{l_W}\left(\frac{q_l}{q_0}\right)_W +$$

$$\left(C_{N_\alpha}\right)_{BT-B}\left(\alpha_{l_T} - \epsilon_{W_e}\right)\left(\frac{q_l}{q_0}\right)_T$$

$$\left(C_m\right)_{total} = \left(C_{m_\alpha}\right)_B \alpha_{l_B}\left(\frac{q_l}{q_0}\right)_B + \left(C_{m_\alpha}\right)_{BW-B} \alpha_{l_W}\left(\frac{q_l}{q_0}\right)_W +$$

$$\left(C_{m_\alpha}\right)_{BT-B}\left(\alpha_{l_T} - \epsilon_{W_e}\right)\left(\frac{q_l}{q_0}\right)_T$$

[redacted]

$$\left(C_Y\right)_{total} = \left(C_{Y_\beta}\right)_B \beta_{l_B}\left(\frac{q_l}{q_0}\right)_B + \left(C_{Y_\beta}\right)_{BW-B} \beta_{l_W}\left(\frac{q_l}{q_0}\right)_W + \left(C_{Y_\beta}\right)_{BT-B} \left(\beta_{l_T} + \sigma_{W_e}\right)\left(\frac{q_l}{q_0}\right)_T$$

$$\left(C_n\right)_{total} = \left(C_{n_\beta}\right)_B \beta_{l_B}\left(\frac{q_l}{q_0}\right)_B + \left(C_{n_\beta}\right)_{BW-B} \beta_{l_W}\left(\frac{q_l}{q_0}\right)_W + \left(C_{n_\beta}\right)_{BT-B} \left(\beta_{l_T} + \sigma_{W_e}\right)\left(\frac{q_l}{q_0}\right)_T$$

The appropriate values of the angle of attack, sideslip, and dynamic pressure were obtained by averaging the local values of α_l, β_l, and $\frac{q_l}{q_0}$ at the approximate centroids of the body nose, the wing, and the tail. The cylindrical portion of the missile body was assumed to carry no force or moment.

As can be seen in figure 12, fair agreement is obtained between the estimated and experimental results for the longitudinal coefficients. In the case of the lateral coefficients, however, although correct qualitative trends are predicted, there exist some large discrepancies in absolute magnitude. One possible reason for these differences may be the fact that the estimation procedure used does not account for any mutual interference effects between the flow fields of the missile and the wing-fuselage combination.

CONCLUDING REMARKS

A low-speed wind-tunnel investigation has been made of some aspects of the aerodynamic problems associated with the use of air-to-air missiles when carried externally on aircraft. Measurements of the forces and moments on a missile model for a range of positions under the midsemispan location of a 45° sweptback wing indicated longitudinal and lateral forces and moments of sufficient magnitude to present possible serious problems with regard to both carriage and release of the missiles. Surveys of the characteristics of the flow field in the region likely to be traversed by the missile showed abrupt gradients in both flow angularity and in local dynamic pressure. Through the use of aerodynamic data on the isolated missile and the measured flow-field characteristics, the longitudinal forces and moments acting on the missile while in the presence of the wing-fuselage combination could be estimated with fair accuracy. Although

the lateral forces and moments predicted were qualitatively correct, there existed some large discrepancies in absolute magnitude.

Langley Aeronautical Laboratory,
National Advisory Committee for Aeronautics,
Langley Field, Va., October 5, 1954.

[redacted]

REFERENCES

1. Luce, R. W., Jr., and Velton, E. J.: Investigation of the Aerodynamic Interference of a Launching Aircraft on the Sparrow II Missile. Rep. No. SM-14383 (Bur. Aero. Contract Na(S)51-252), Douglas Aircraft Co., Inc., Oct. 29, 1952.

2. Evans, K. E., and Freeman, P. A.: Launch Study Supplement XAAM-N-4 (Oriole) Launching Dispersions Including the Effects of the Airplane Wing and Pylon on the Flow Field Around the Missile. Eng. Rep. No. 5058 (Contract NOa(S)51-194-C), The Glenn L. Martin Co., Apr. 1952.

3. Silvers, H. Norman, and King, Thomas J., Jr.: Investigation at High Subsonic Speeds of Bodies Mounted From the Wing of an Unswept-Wing–Fuselage Model, Including Measurements of Body Loads. NACA RM L52J08, 1952.

4. Alford, William J., Jr., and Silvers, H. Norman: Investigation at High Subsonic Speeds of Finned and Unfinned Bodies Mounted at Various Locations From the Wings of Unswept- and Swept-Wing–Fuselage Models, Including Measurements of Body Loads. NACA RM L54B18, 1954.

5. Silvers, H. Norman, and Alford, William J., Jr.: Investigation at High Subsonic Speeds of the Effect of Adding Various Combinations of Missiles on the Aerodynamic Characteristics of Sweptback and Unswept Wings Combined With a Fuselage. NACA RM L54D20, 1954.

6. Gillis, Clarence L., Polhamus, Edward C., and Gray, Joseph L., Jr.: Charts for Determining Jet-Boundary Corrections for Complete Models in 7- by 10-Foot Closed Rectangular Wind Tunnels. NACA WR L-123, 1945. (Formerly NACA ARR L5G31.)

7. Herriot, John G.: Blockage Corrections for Three-Dimensional-Flow Closed-Throat Wind Tunnels, With Consideration of the Effect of Compressibility. NACA Rep. 995, 1950. (Supersedes NACA RM A7B28.)

[redacted]

TABLE I.- FUSELAGE ORDINATES

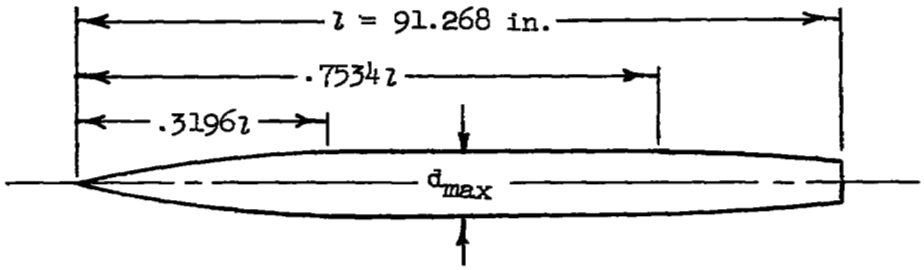

Ordinates, percent length	
Station	Radius
0	0
3.28	.91
6.57	1.71
9.86	2.41
13.15	3.00
16.43	3.50
19.72	3.90
23.01	4.21
26.29	4.43
29.58	4.57
75.34	4.57
76.69	4.54
79.98	4.38
83.26	4.18
86.55	3.95
89.84	3.72
93.13	3.49
96.41	3.26
100.00	3.02

[redacted]

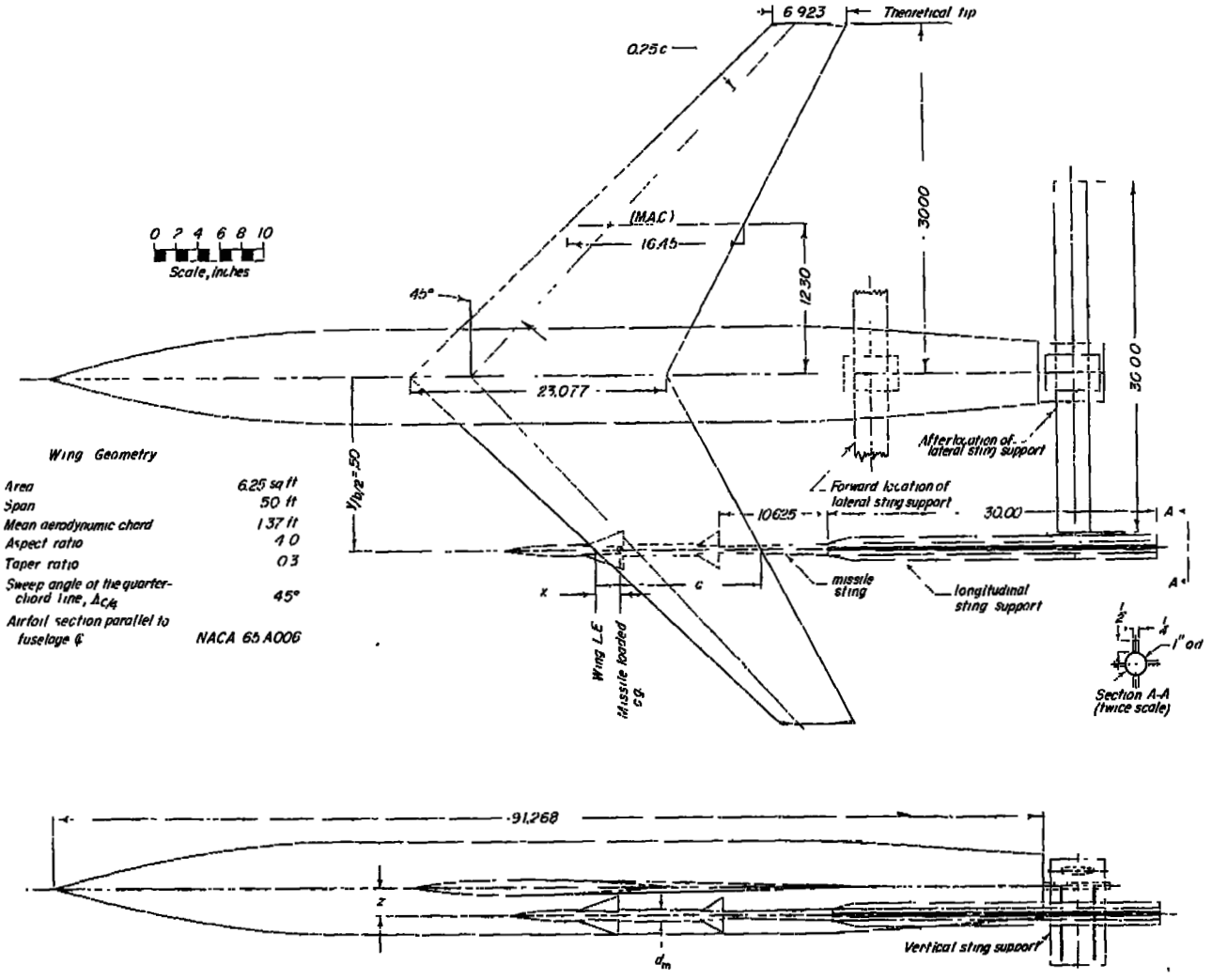

Figure 1.- Test setup showing the missile in one test location. (All dimensions are in inches unless otherwise noted.)

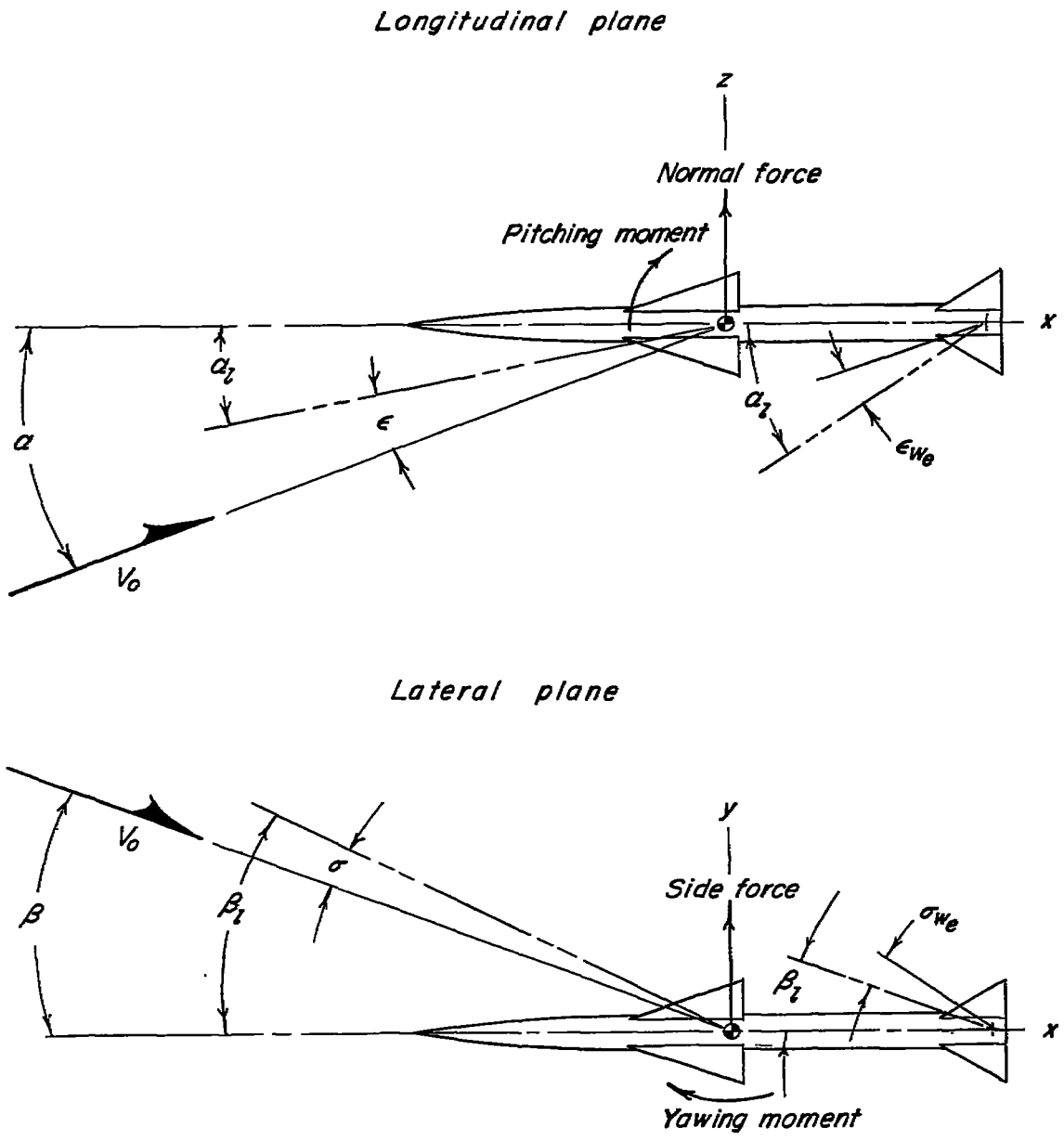

Figure 2.- Positive directions of forces, moments, and angles.

[redacted]

L-80760.1

Figure 3.- Photograph of model with angularity rake installed.

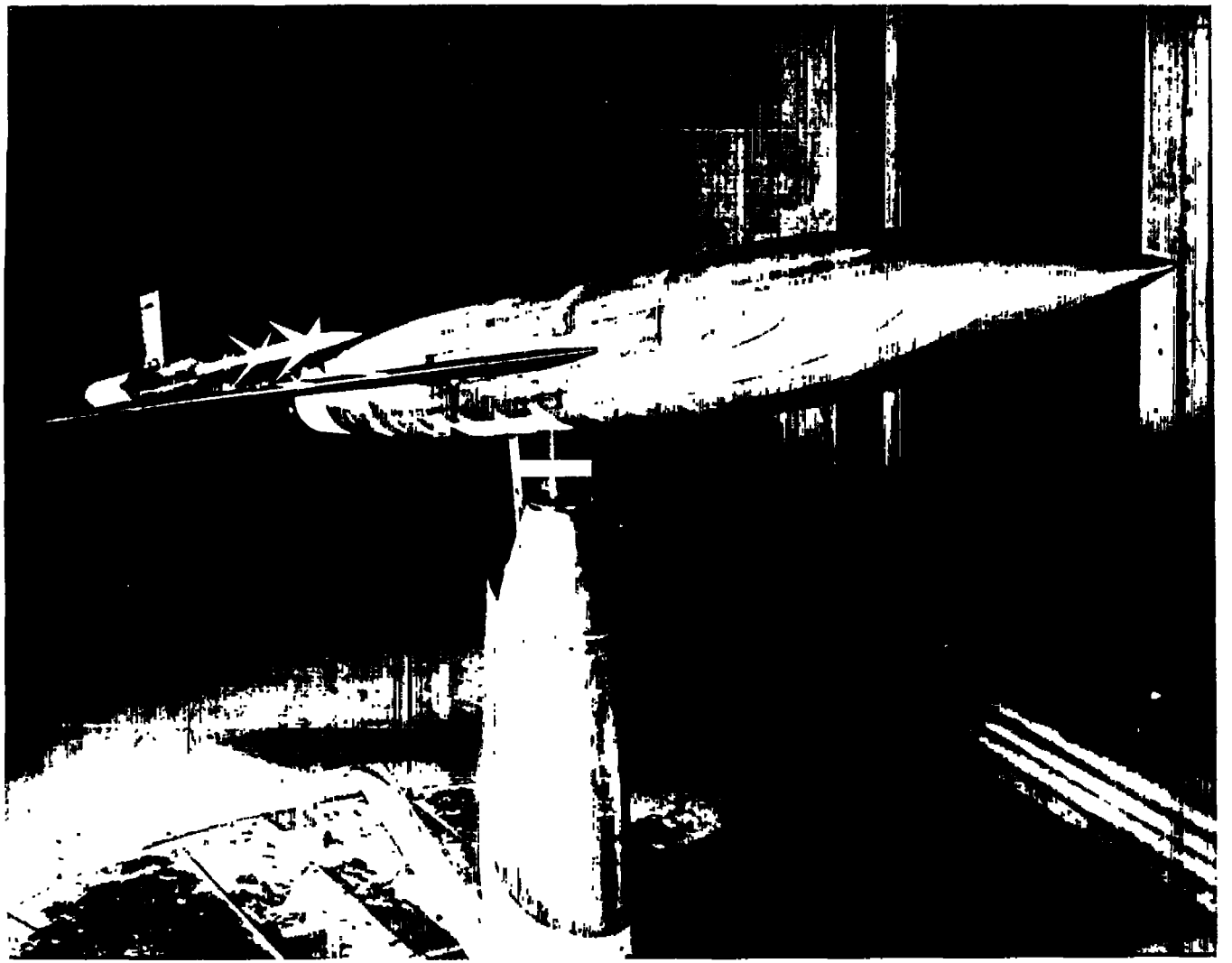

L-82628

Figure 4.- Photograph of model with missile installed.

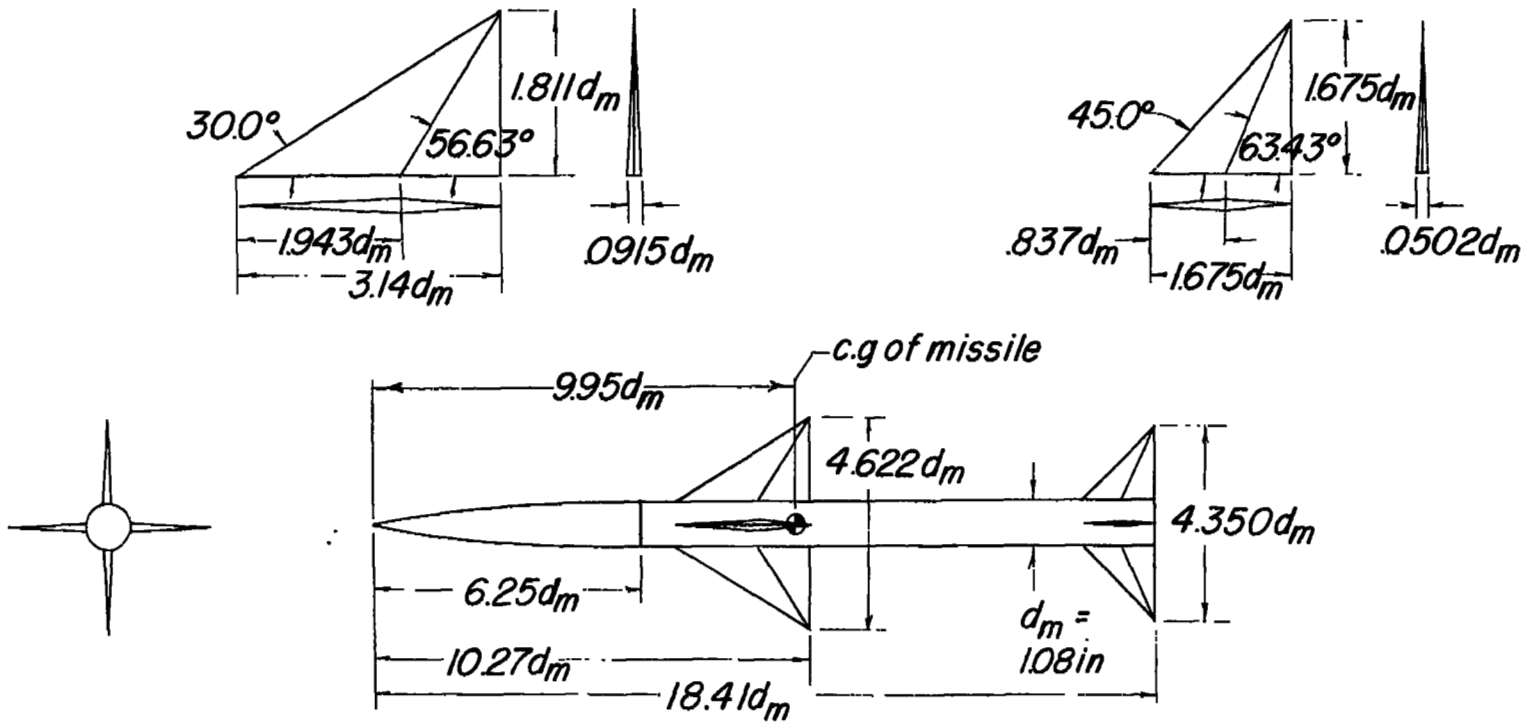

Figure 5.- Drawing of missile model showing general dimensions.

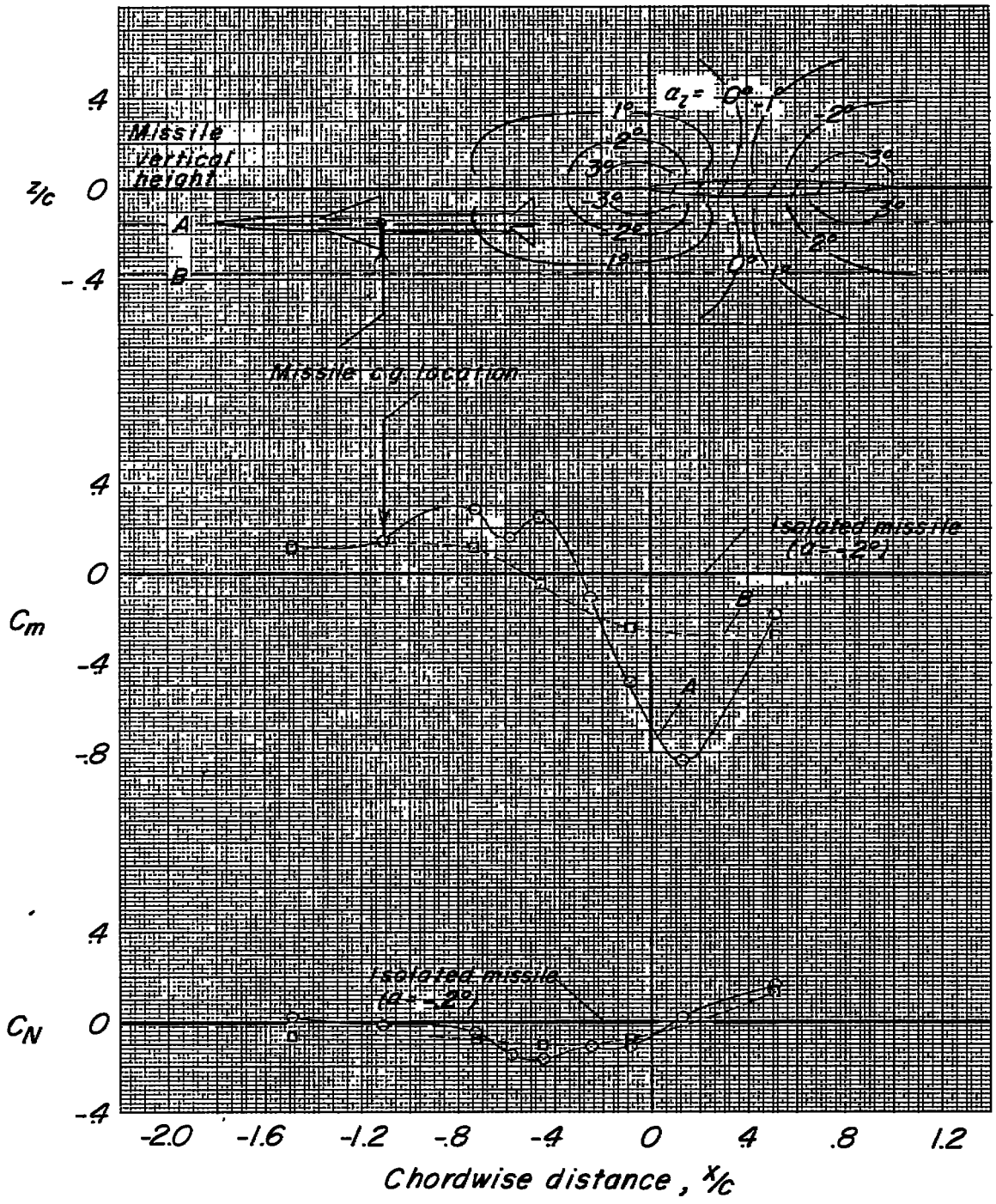

(a) Longitudinal characteristics.

Figure 6.- Angularity contours and missile forces and moments for $\alpha = -0.2^{\circ}$; $\beta = 0^{\circ}$.

[redacted]

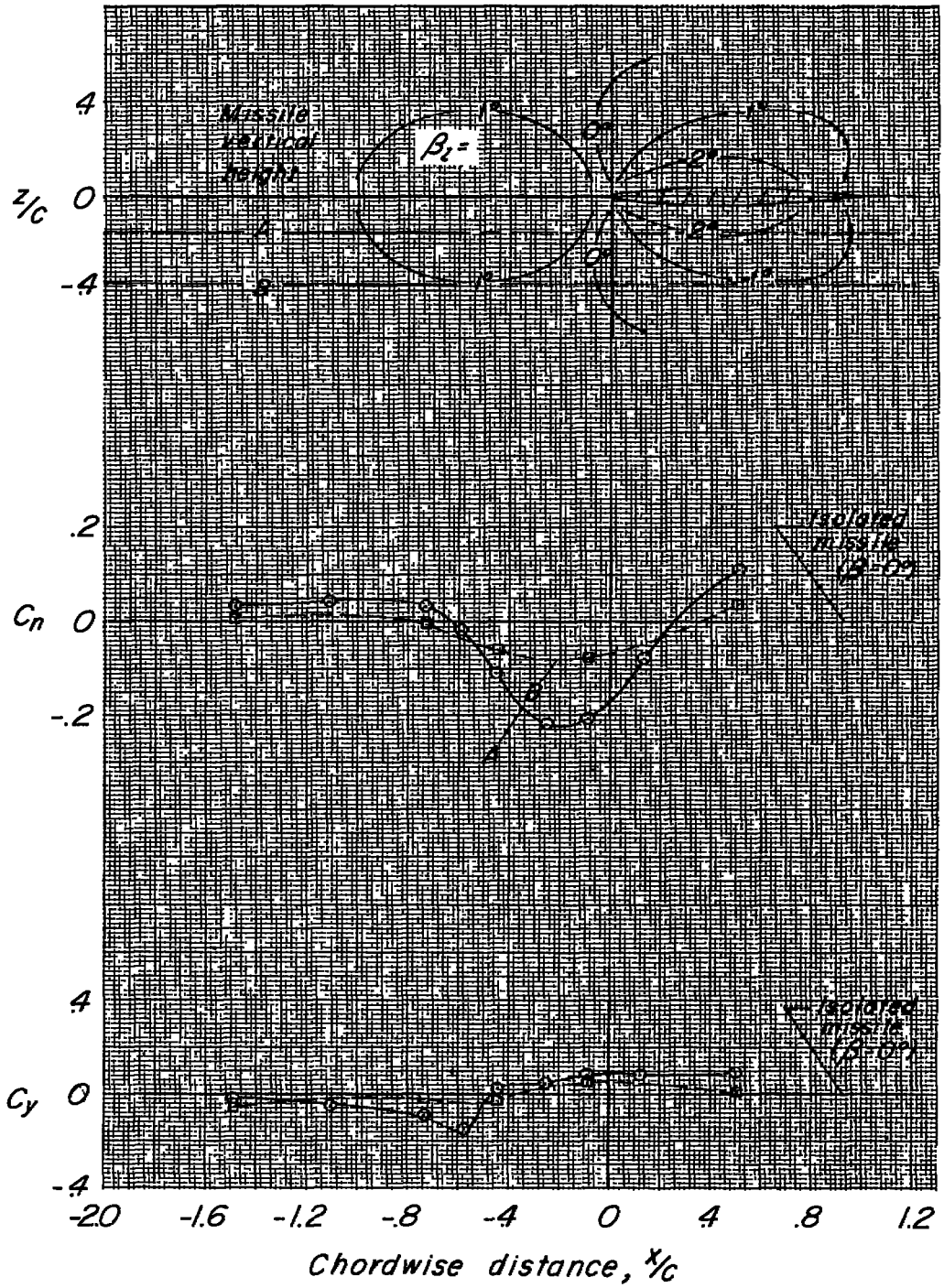

(b) Lateral characteristics.

Figure 6.- Concluded.

[redacted]

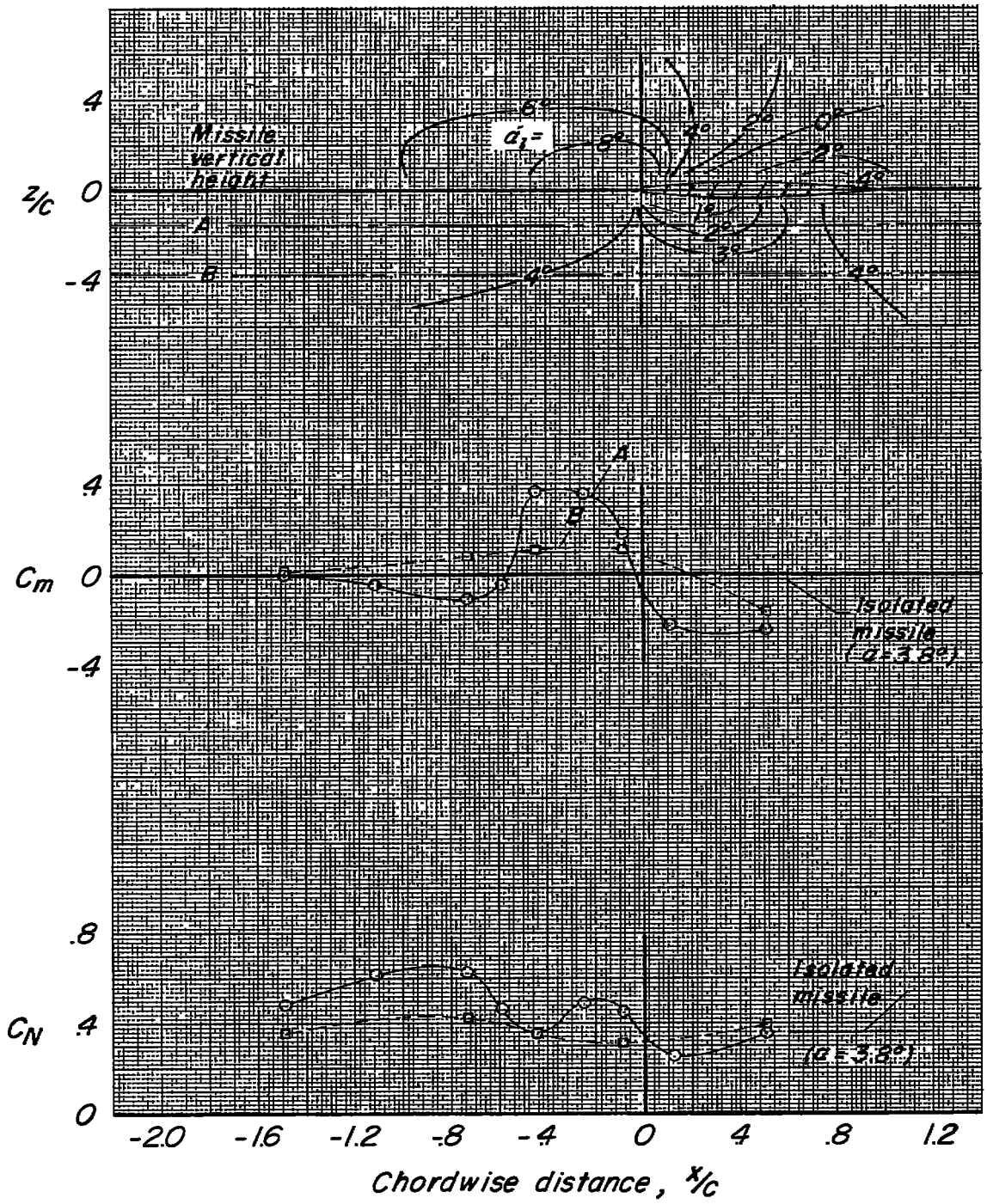

(a) Longitudinal characteristics.

Figure 7.- Angularity contours and missile forces and moments for $\alpha = 3.8^{\circ}$; $\beta = 0^{\circ}$.

[redacted]

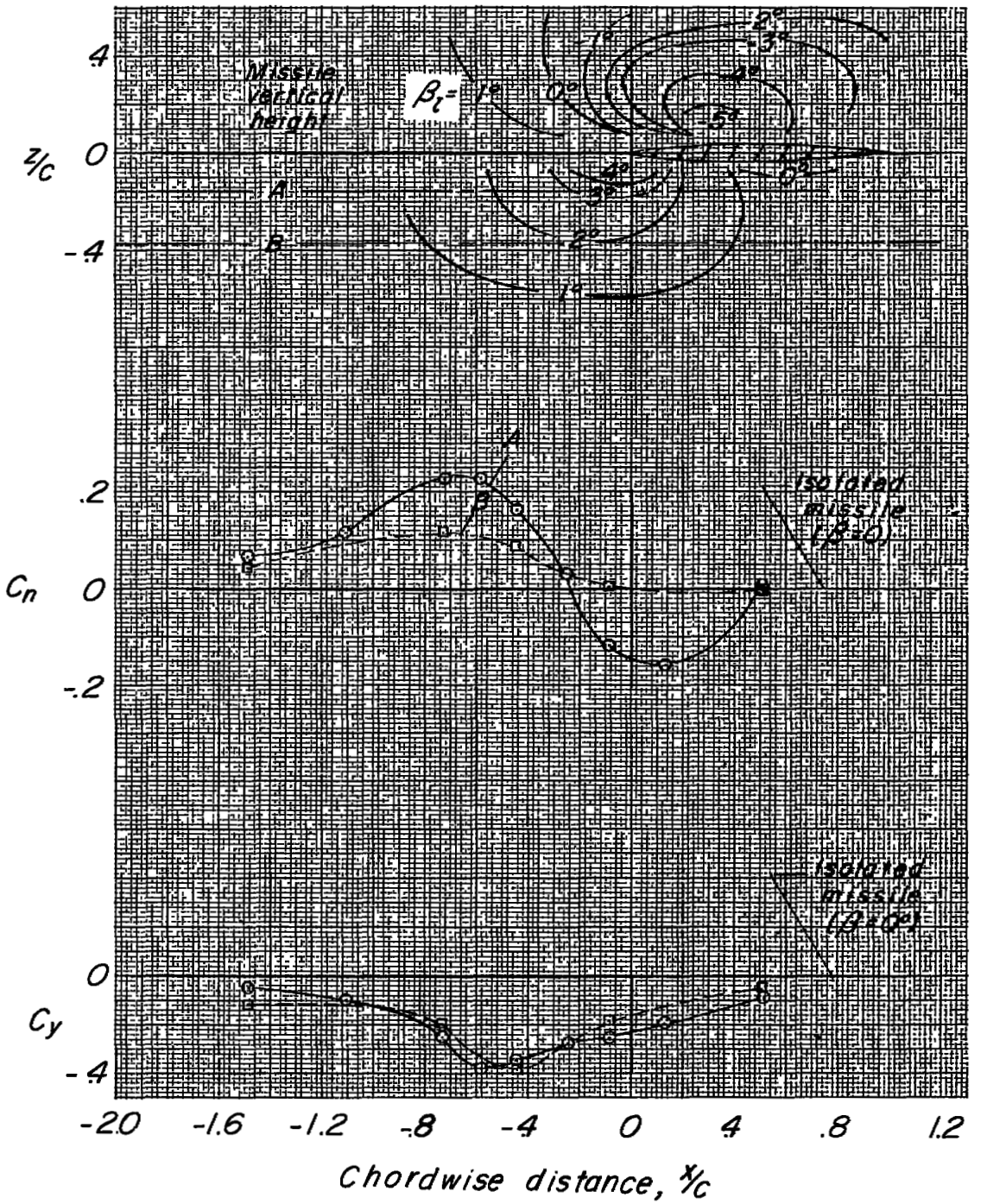

(b) Lateral characteristics.

Figure 7.- Concluded.

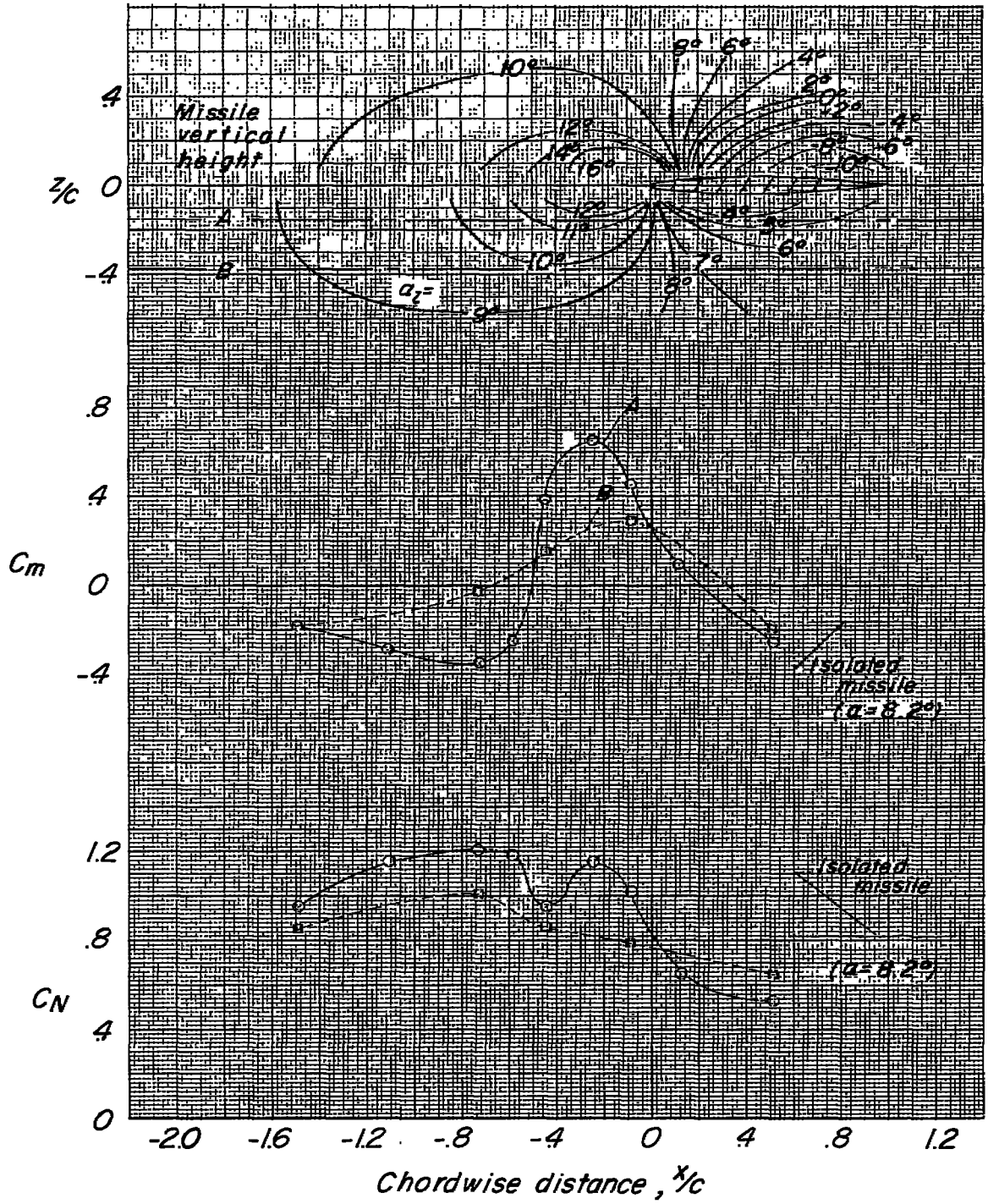

(a) Longitudinal characteristics.

Figure 8.- Angularity contours and missile forces and moments for $\alpha = 8.2^{\circ}$; $\beta = 0^{\circ}$.

[redacted]

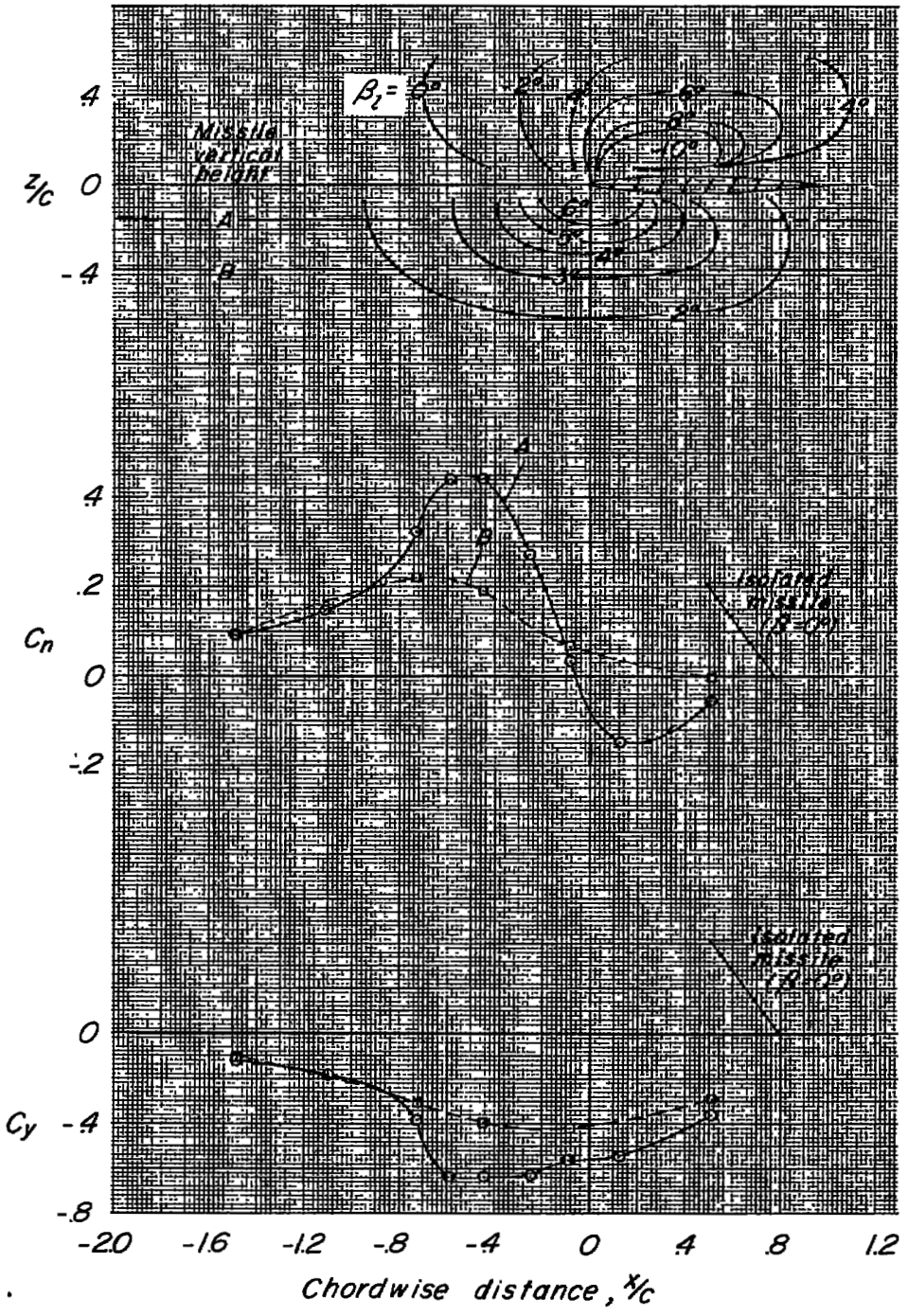

(b) Lateral characteristics.

Figure 8.- Concluded.

[redacted]

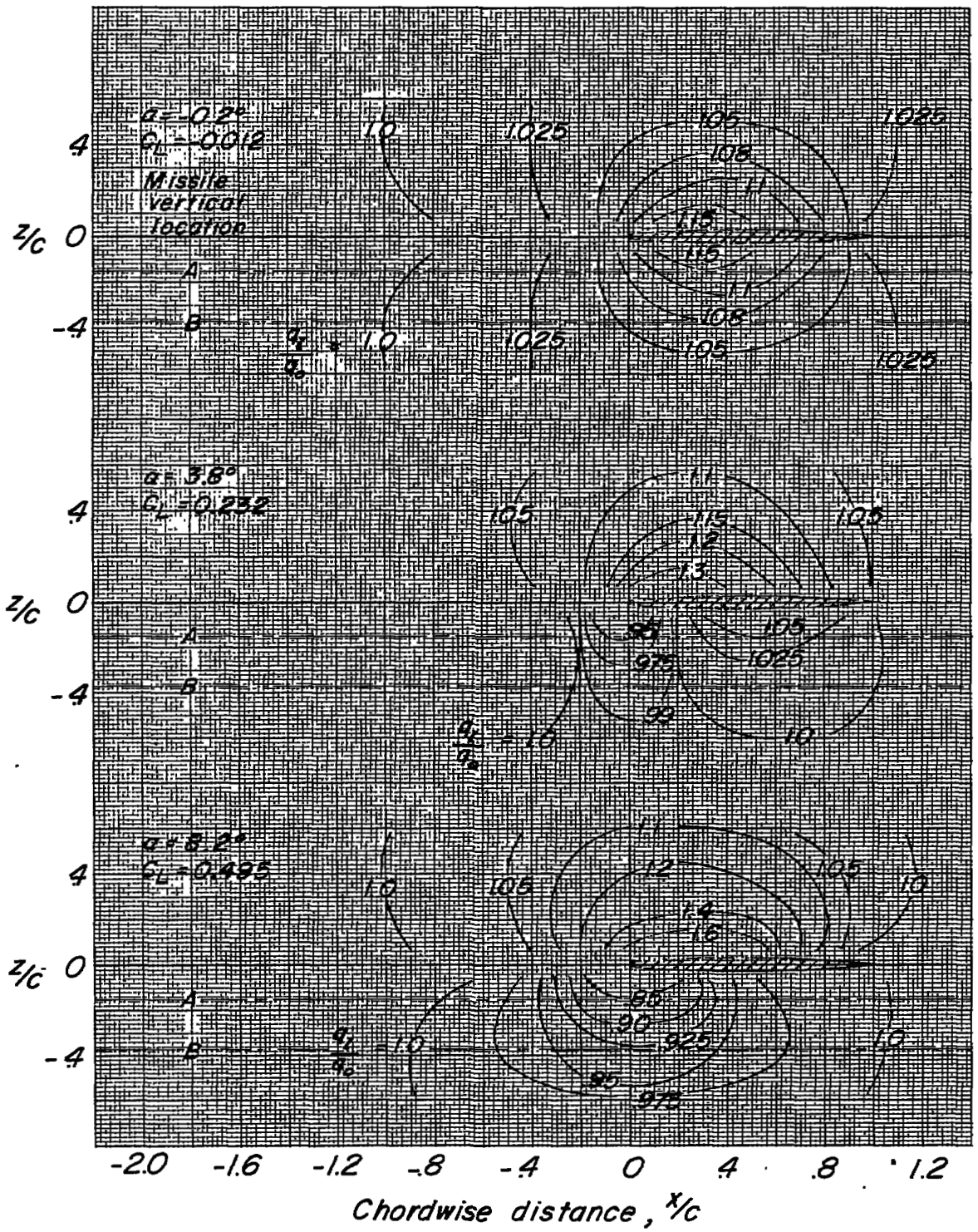

Figure 9.- Dynamic-pressure ratios for several angles of attack.

[redacted]

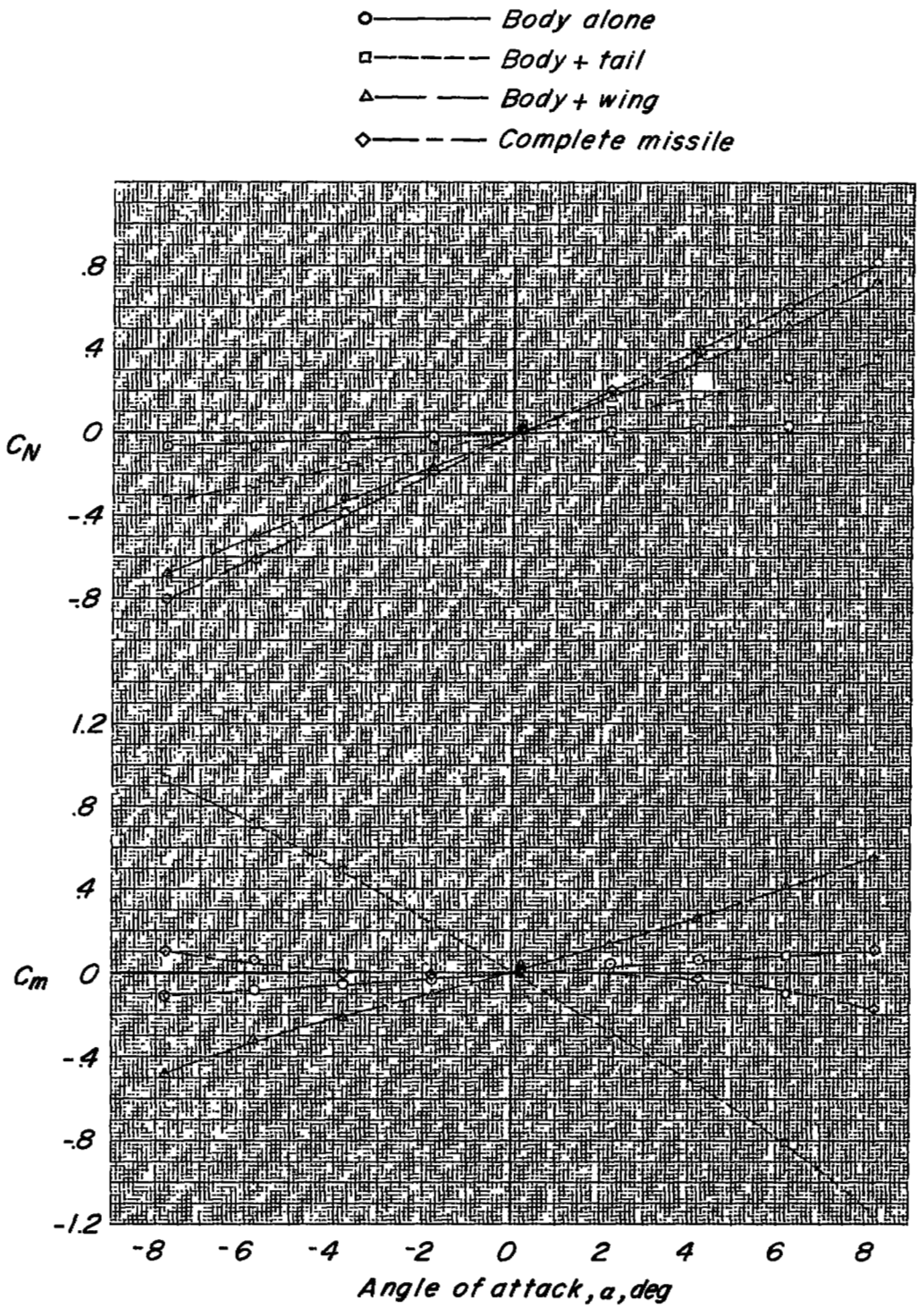

Figure 10.- Force and moment characteristics of isolated missile.

[redacted]

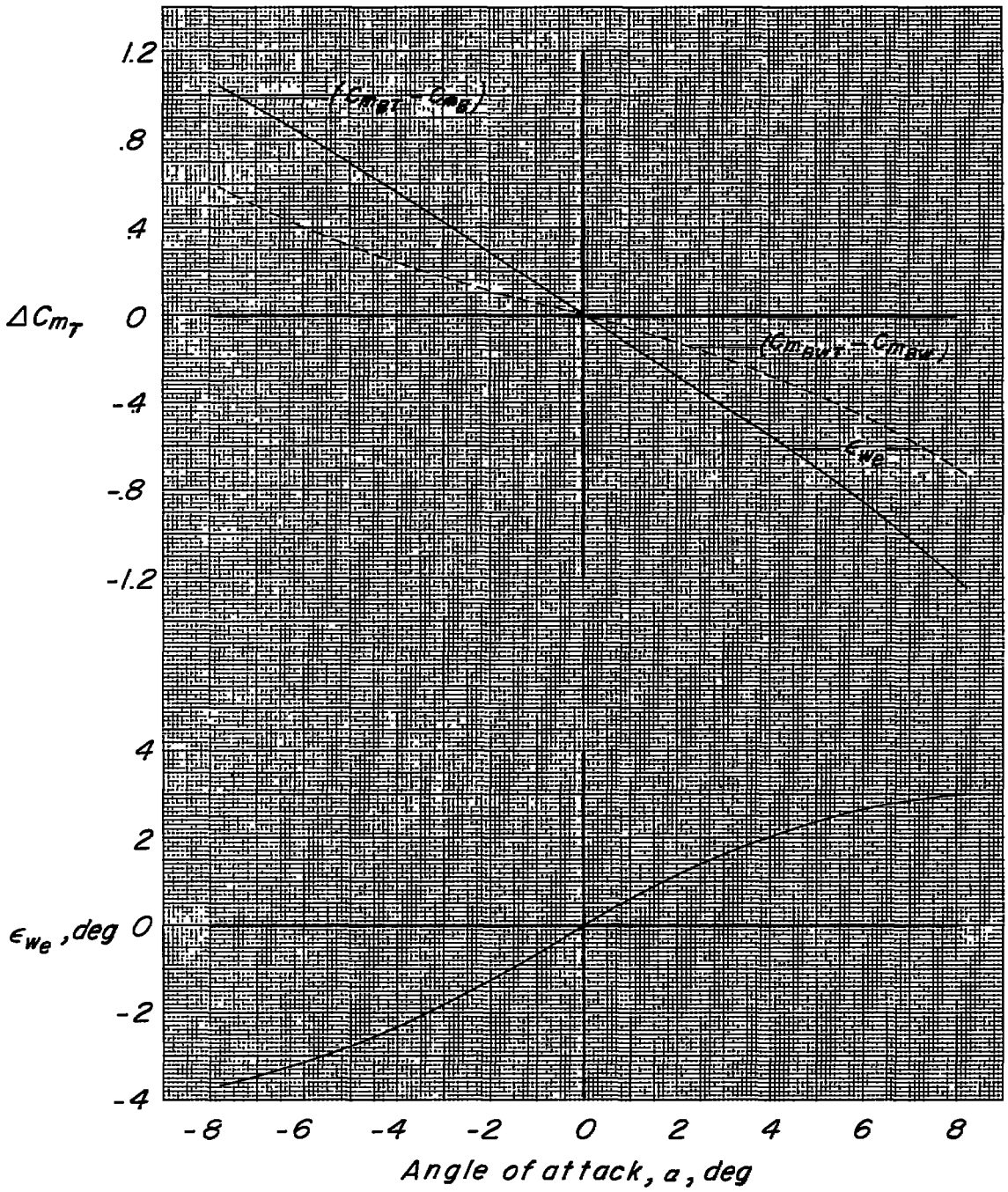

Figure 11.- Downwash characteristics of isolated missile.

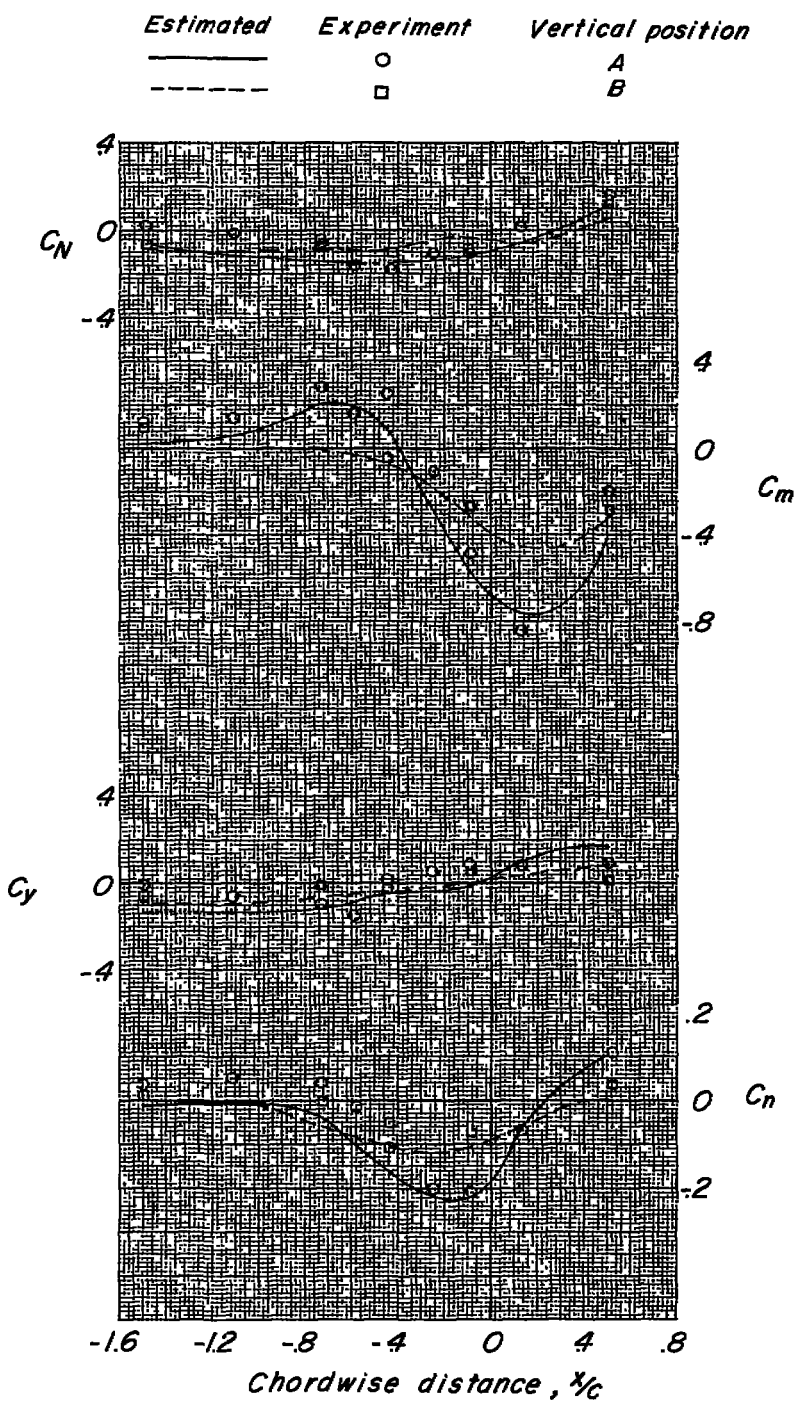

(a) $\alpha = -0.2^{\circ}$; $\beta = 0^{\circ}$.

Figure 12.- Comparison between estimated and experimental missile forces and moments.

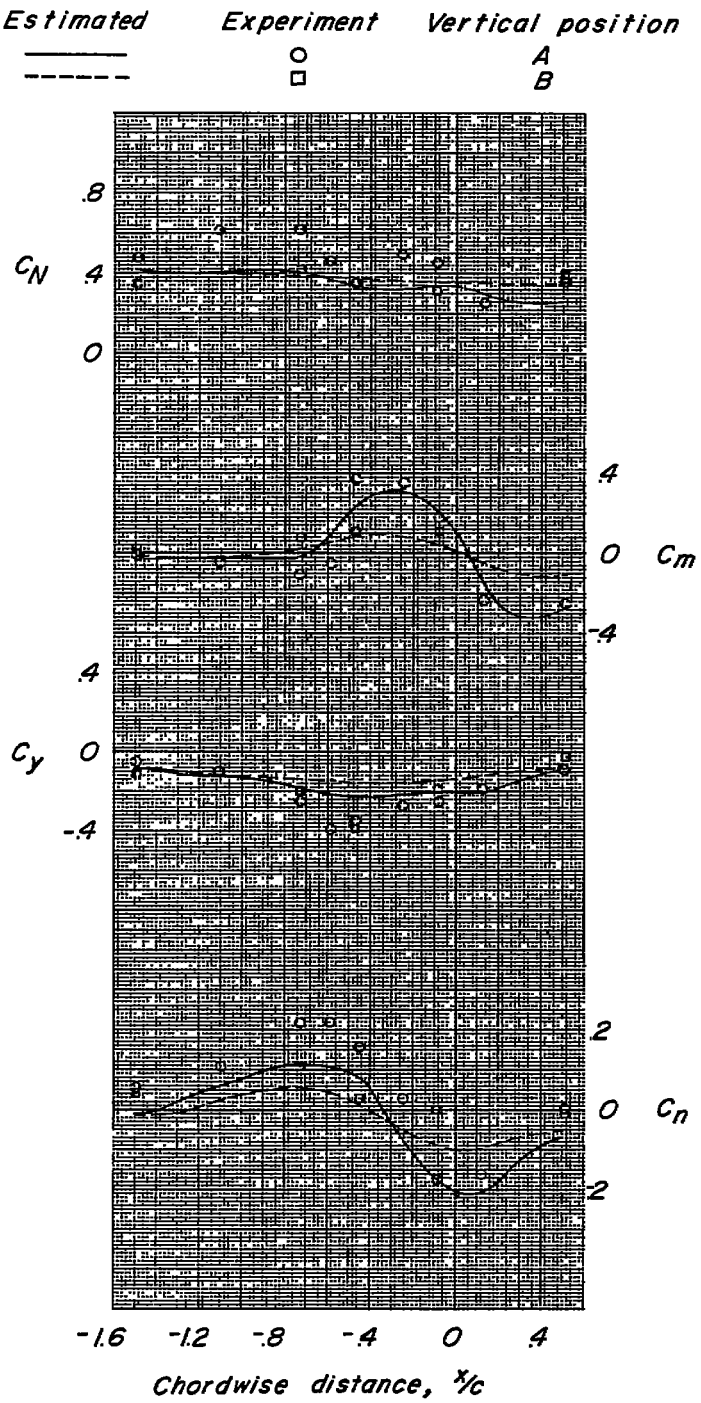

(b) $\alpha = 3.8^\circ$; $\beta = 0^\circ$.

Figure 12.- Continued.

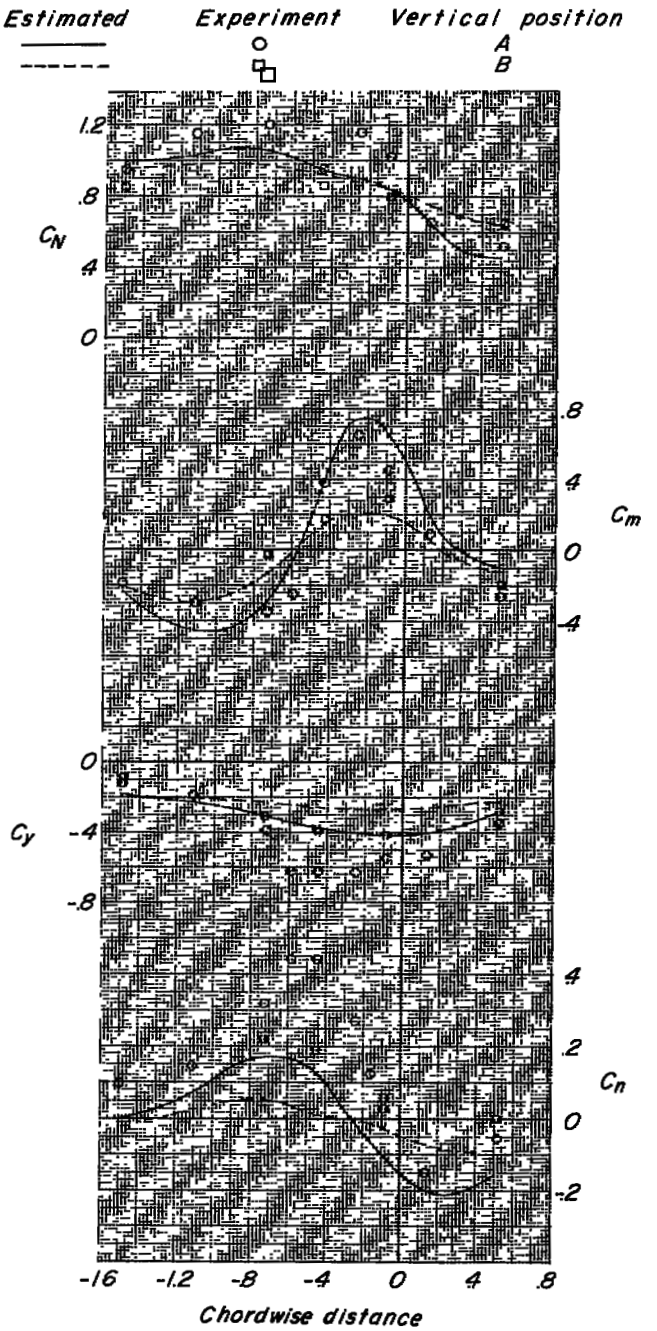

(c) $\alpha = 8.2^\circ$; $\beta = 0^\circ$.

Figure 12.- Concluded.